

IPC00-0031

REVIEW OF CTOA AS A MEASURE OF DUCTILE FRACTURE TOUGHNESS

L.N. Pussegoda^[1], S. Verbit^[1], A. Dinovitzer^[1], W. Tyson^[2], A. Glover^[3], L. Collins^[4], L. Carlson^[5],
J. Beattie^[6]

[1] Fleet Technology Limited, Kanata, Ontario, Canada

[2] MTL, CANMET, NRCan, Ottawa, Ontario, Canada

[3] TransCanada Pipelines Limited, Calgary, Alberta, Canada

[4] Ipsco, Regina, Saskatchewan, Canada

[5] Alliance Pipelines, Calgary, Alberta, Canada

[6] Foothills Pipe Lines, Calgary, Alberta, Canada

ABSTRACT

The ductile fracture toughness of steel is used to assess the ability of a pipeline to resist long running ductile fractures in a burst event. With the introduction of modern low carbon clean steels with ultra high toughness, conventional measures of ductile fracture toughness (standard Charpy and DWTT energy) are under review, and alternatives are being studied. The crack tip opening angle (CTOA) was investigated to evaluate its appropriateness as a measure of modern pipeline steel ductile fracture toughness. At first, fracture mechanics tests at quasi-static rate were analyzed to examine the constancy of CTOA with crack growth. The results of this initial review are based on four pipeline steels with a range of ductile fracture toughness. The CTOA values are also compared with appropriate parameters from conventional tests to examine potential relationships that may be used to indicate the relative resistance of pipeline steels to ductile fracture propagation. The final objective is to compare CTOA values determined by the simple two specimen method and those developed through a formal fracture mechanics based technique.

INTRODUCTION

Design against long ductile fracture propagation in gas pipelines involves an analysis of the balance between driving force, derived from the gas pressure, and the fracture resistance of the material. Initially, the shelf energy in the Charpy test was successfully used as a measure of fracture propagation resistance. As material strength, pipe diameter and operating pressure increased, requiring greater fracture propagation resistance, the limitations of the Charpy energy approach became increasingly apparent [1]. This is because for modern steels, the Charpy test involves significant energy absorption contributions from processes not related to fracture propagation. Various attempts have been made to extend the

range of applicability of the Charpy energy, and to develop alternative approaches more directly related to the propagation process. If an energy-balance approach is to be maintained, and if material resistance is to be measured in a fairly simple laboratory notch bend test (e.g., Charpy or drop-weight tear), the problem reduces to the isolation of the propagation energy absorption per unit of crack advance. Results of such an approach are reported at this conference [2].

Crack tip opening angle (CTOA), which is a formal fracture mechanics based parameter, has been considered as a measure of resistance to ductile fracture propagation. It has been claimed that CTOA is constant during steady state crack propagation [3,4] and therefore has the promise of being directly applied to full-scale pipeline fracture. The CTOA may be a viable alternative to the Charpy energy for characterizing fracture, and therefore has particular promise for modern high strength linepipe where the significance of the Charpy energy is increasingly coming under question.

The present investigation is focused on evaluating the variation of CTOA with crack growth in a SENB type specimen. The effect of ligament size on CTOA is also studied using non-standard shallow notched SENB specimens. Four modern low C, low S chemistries and thermo-mechanically controlled processed (TMCP) steels, were selected for study.

STEEL CHARACTERIZATION

Table 1 lists the Grade and dimensional information on the pipes. The pipes were supplied by the sponsors of this program. The objective of this task is material comparison, employing standard methods.

Small tensile specimens (gauge diameter of 5 mm and gauge length of 25 mm) were extracted in the circumferential orientation and tested at a quasi-static rate ($0.0001s^{-1}$) and a higher rate ($2s^{-1}$). The properties that are expected to relate to CTOA are true strain at fracture (ϵ_t)

and area under the true stress vs. true strain curve (A). Figure 1 displays the features of the curve. A polynomial of the second order was used to fit a curve from the point of plastic instability to fracture, to obtain an approximate measure of the strain energy density for fracture.

Table 2 displays the tensile properties of the steels and the corresponding derived data at the two rates of testing. The expected strain rate sensitivity is observed for the yield strength, fracture strain and strain energy density, i.e., the yield strength is raised while the other two parameters drop with increase in the strain rate. However, steel 4840-2 shows an unexpected increase in the fracture strain at the higher rate of testing.

The microstructure of steels 4840-1 and 4840-2 displays a large proportion of ferrite that is elongated in the rolling direction especially in 4840-1 (Figure 2a). The

second phase, not resolved at optical magnifications, doubtless consist of low temperature transformation products. By contrast, the other two steels have acicular ferrite with very little second phase (Figure 2b – 4840-3).

The Charpy transition curves for two steels are presented in Figure 3. Specimens from steels 1, 2 and 3 all display splitting in planes parallel to the plate surface. As the test temperature is raised the extent of splits is reduced with a corresponding increase in the absorbed energy, thus demonstrating rising upper shelf (RUS) behaviour. For steels 1 through 3, in the fracture transition range the cleaved planes are at an angle to the mode I fracture plane. In the lower shelf of the transition the fracture is of the conventional cleavage type (mode I). By contrast, steel 6 shows a sudden ductile/brittle transition between -45°C and -65°C .

Table 1: Selected Steel Pipes

Pipe steel ID	Grade	Diameter mm (inches)	Thickness mm (inches)	Steel origin
4840-1	X70	914 (36)	14.2 (0.559)	Canada
4840-2*	X70	1067 (42)	12.0 (0.472)	Canada
4840-3	X80	1219 (48)	15.3 (0.602)	Canada
4840-6	X70	914 (36)	12.0 (0.472)	Canada

- vintage early 1980

Table 2: Tensile Properties of the Steels and Derived Data

Steel	0.2% Y.S. (MPa)	UTS (MPa)	Elongation (%)	ϵ_u	ϵ_f	A, (MPa)
Quasi-static strain rate						
4840-1	579	652	22.3	0.074	1.60	2617
4840-2	554	684	24.6	0.094	0.92	1023
4840-3	564	677	25.0	0.122	1.46	1810
4840-6	520	624	26.7	0.085	1.67	2849
Impact strain rate						
4840-1	626	696	22.1	0.095	1.31	1823
4840-2	601	721	25.8	0.122	1.14	1603
4840-3	597	720	24.7	0.111	1.27	1427
4840-6	559	661	27.5	0.121	1.49	2445

ϵ_u is uniform elongation

The curved DWTT specimens extracted from the pipe were “straightened” to ensure that the load point and support points were in the same plane to obtain fracture along the pipe axis. A modified procedure, following the guidelines in BS 7448: Part II: 1997 [5], was used with the objective of avoiding any plastic deformation along the intended fracture plane. The specimens were tested at room temperature, and the load-displacement data was used to determine the total (standard) energy required for fracture and the portion of that energy consumed after peak load. Figure 4 shows that the steels selected display a range of absorbed energies, and also the post peak energy is

about 2/3 of the total energy for these steels. The total energy absorbed during specimen fracture has a large contribution from deformation not related to fracture propagation [1,2].

Testing was performed on (B x 2B, B – wall thickness) SENB type specimens to obtain resistance curves following the ASTM E1820-96 approach. The specimens were, however, non-standard as they were straightened similar to the DWTT specimens with the same objective. The validity criterion for initial (fatigue) crack straightness, using the 9-point average, was met.

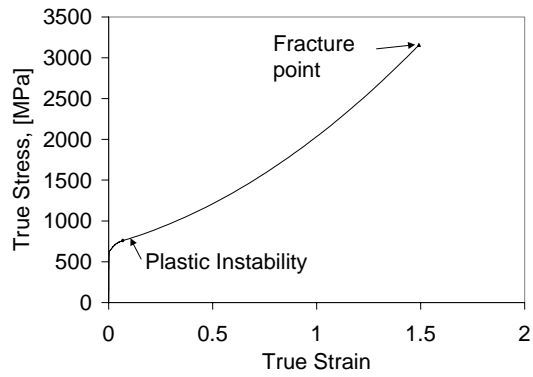


Figure 1: True Stress vs. True Strain Curve up to Plastic Instability and Its Extension up to Fracture

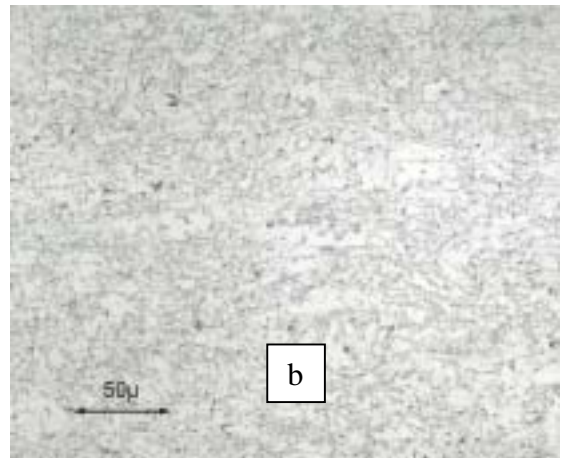
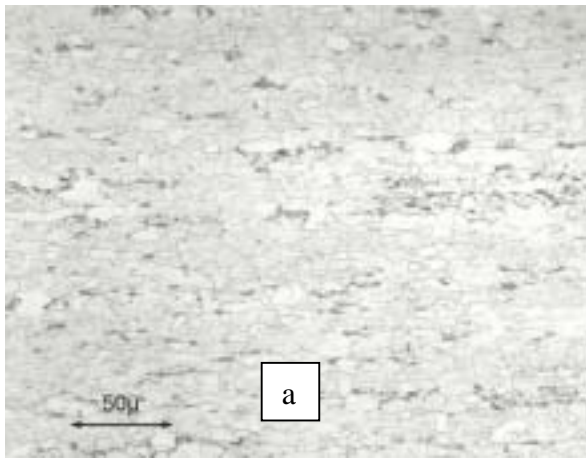


Figure 2: Microstructures of Steels (a) 4840-1 and (b) 4840-3 at (X400), with Arrow of the Micron Marker Indicating the Major Rolling Direction.

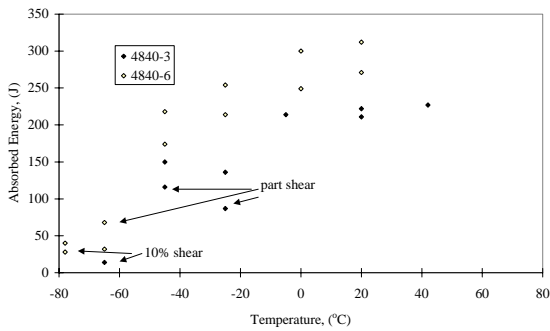


Figure 3: Charpy Transition Curves for Steels 4840-3 and 4840-6

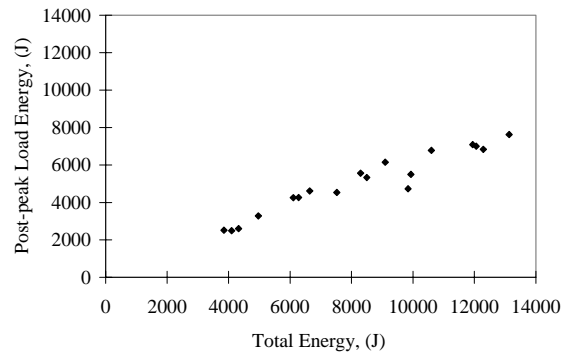


Figure 4: DWTT Energy vs. Post Peak Load Energy for Room Temperature Tests


However, the straightness and predictions for subsequent crack growth at the end of the resistance curve testing were not always met, even though side grooves were machined after fatigue pre-cracking. For steel 3, instability occurred early in the test (i.e., before a 0.2 mm growth) due to splitting and, therefore, a resistance curve was not developed, rather J_{Qc} and δ_c values were determined. Since the data requirements for J_{Ic} determination in accordance with ASTM E 1820 were not met, the J and δ (average of three) at a total predicted crack extension (Δa) of 0.4 mm were measured and are reported in Table 3.

Table 3: Results from Initiation Tests

Steel	J , (kJ m ⁻²)	δ , (mm)
4840-1	300	0.23
4840-2	200	0.22
4840-3*	265	0.21
4840-4	275	0.25

* J_{Qc} and δ_{Qc} from a single specimen that gave the earliest event

QUASI-STATIC CTOA

The primary objective of this task was to examine CTOA constancy  crack growth and specimen (ligament) size variation using 3-point bend specimen. The tests were performed at room temperature.

The investigation aimed at crack propagation beyond the 2 mm crack extension where the growth of a fully developed crack is the focus, as CTOA is known to decrease during the initial crack growth. Therefore, a fatigue crack is not necessarily a starting point as in the previous task where the focus is the resistance to initiation. Another variant from the initiation test is the absence of side grooves so that a full thickness crack would be evaluated and hence it was envisaged that the crack front will not be straight. The specimens were chevron notched using a 1.6 mm (1/16 inch) milling cutter with a sharp radius at the root. The included angle of the chevron is 90°. The effect of ligament size was evaluated using (B x 2B), (B x 4B) and (B x 6B) specimens each having a chevron notch of depth B measured at the specimen surface. The specimens were straightened as before.

The test was performed in two stages, statically pre-cracking (PC) followed by testing using the method adopted by Turner and co-workers [3,6]. For the first stage, the specimens were loaded monotonically beyond the limit load with the aim of getting a fully developed crack in the chevron region. To achieve this consistently, it was necessary to proceed to a specified load beyond peak load for each specimen size, for example, for the (B x 2B) specimen the load was about 85% of the peak load. With the increase in specimen ligament size, this percentage of peak load had to be increased up to 97% in the (B x 6B) size to get the same crack growth. The Turner approach of

performing the test is essentially the same as the standard method. The difference is that the crack extension is continued further, relative to the original unbroken ligament, and thus it far exceeds the specimen capacity given in ASTM E1820. Loading rate was adjusted so that the peak load in this second stage was reached in ≈ 60 s, and this is at the higher end of large range allowed in ASTM E 1820.

J-Resistance Plots

J-R plots were derived from the data gathered during the propagation stage. The main objective of this stage of testing is to evaluate the CTOA with crack extension. In Figure 6, a typical J-R plot for steel 4840-2 is shown. Note that this is developed from the portion of the load-displacement beyond the peak load, and so, it is different from the conventional J-resistance curve. In the figure, J vs. Δa data from three methods are presented and summarized in the legend. JR from flex, is the standard method where a flex bar mounted on the specimen is used to measure load line displacement, and JR from CMOD [7] is being proposed as an improved method for CTOD determination currently being considered in ASTM committee E8. The crack length predictions are made both from elastic compliance during periodic unloading and direct current potential drop (DCPD) methods.



Figure 5: Test Set Up

Figure 7 is presented to display typical crack length predictions from the two methods for comparison with results in Figure 6. Results show that the PD method gives a more reliable crack length prediction at the early stages of growth than the compliance based calculations. This

provides evidence of the relative insensitivity of elastic compliance, to length changes, at shallow crack depths.

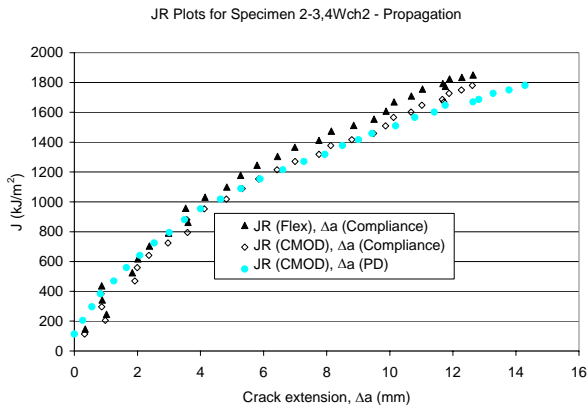


Figure 6: Typical J-R Plot for Steel 4840-2, Specimen Size (B x 4B) for the Propagation Stage

The crack length estimates made from elastic compliance measurements were expected to be inaccurate, considering the insensitivity of the specimen compliance at shallow crack depths [8]. For the (B x 4B) size, the a_0/W ratio is 0.25 and for (B x 6B) it is 0.17, as a_0 for both specimen sizes is B (wall thickness of the pipe). Figure 7 demonstrates a worse case scenario of this inaccurate prediction as demonstrated by the scatter.

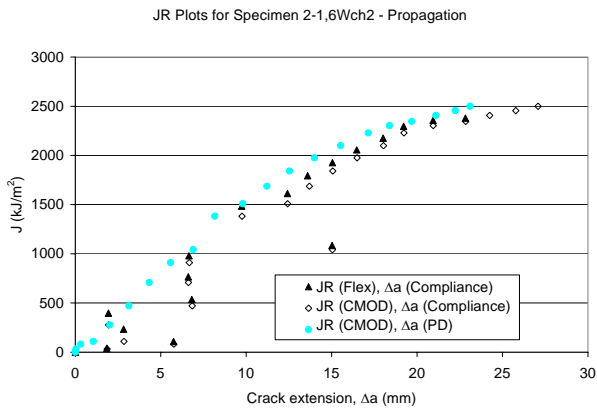


Figure 7: J-R Plot for Steel 4840-2, Specimen Size (B x 6B) for the Propagation Stage

Selected specimens were heat tinted to mark the crack advance and broken open at low temperature, after completing the tests. Figure 8 shows the fractures from steels 2 and 3; the heat tinted region in steel 3 displays splits. Further, as expected, crack shape was non-uniform with more growth in the center. The fractures show significant plastic deformation, and these features are different compared to a standard J test in a side grooved specimen. The crack extension predictions, using the

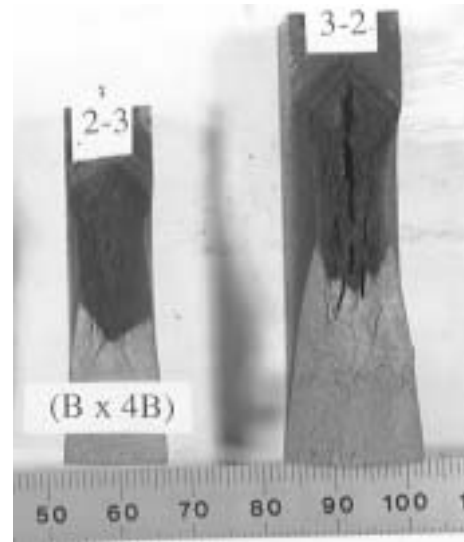


Figure 8: Fractures from (B x 4B) specimens

DCPD approach, were based on calibrations performed using the measured final crack length taken at the quarter thickness location. The calibration was normalized to account for the different thickness of the steels. The calibration and the subsequent prediction were performed from the change in PD after the PC process, eliminating the changes in PD caused by plastic deformation during the formation of the initial crack. When comparing predictions with measured values, it should be noted at the outset, that the compliance method uses elastic compliance equations from ASTM E1820, whereas for PD prediction, calibration using measured crack lengths are employed as described above. The compliance method was found to consistently under-predict the final crack length by about 10 to 15%, as expected from the crack shape, with more growth in the center. The PD method was found to be reliable when the actual crack lengths were similar to those used for calibration, however, extension of the calibration outside its range proved to be less accurate.

CTOA Calculations

Figures 9a and 9b are shown to display the concept of the crack opening angle (COA) in two specimens that were tested. These figures show how the specimen arms rotate about a center of rotation in the ligament. Expressions for the crack tip opening angle (CTOA), defined as $(\Delta\delta/\Delta a)$, where δ is the crack tip opening displacement (CTOD), have been developed using this concept of a point of rotation, by a number of authors [6,9,10]. For small half rotation angles (i.e., angle of rotation of one arm, with $\tan(\theta) = \theta$), CTOA was obtained following Turner [3,6]:

$$\frac{dq}{da} = \frac{S CTOA}{4r_{pl}^*(W-a)} \quad (1)$$

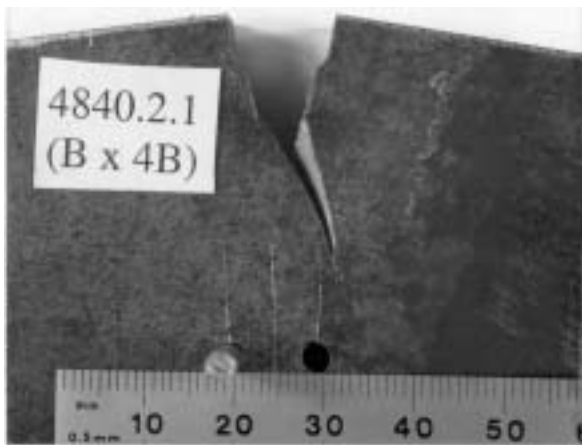
$$q = -\frac{S CTOA}{4r_{pl}^*} \ln(W-a) + C$$

where dq/da is the change in load line displacement (q) with crack length (a), r_{pl}^* is the plastic rotation factor determined from equation 2, b is the ligament length ($W-a$) and S is the span. The rotation factor is determined from [6]:

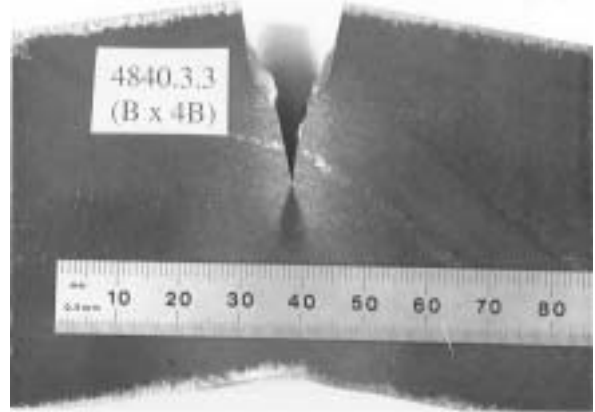
$$r_{pl}^* = \left(\frac{S}{4} \frac{dV_{pl}}{dq_{pl}} - a_o \right) / b_o \quad (2)$$

where dV_{pl}/dq_{pl} is determined from the slope of the plastic CMOD vs. plastic load line displacement curve. The rotation factor, defined as the ratio of the distance of the crack tip to the point of rotation of the specimen arms to the ligament length, is nominally around 0.45 for standard (B x 2B) specimens.

Two examples of the plot of load line displacement (q) vs. $\ln(W-a)$ for (B x 4B) specimens are presented in Figures 10a and 10b, for steel 4840-2, for crack length prediction from compliance and PD method, respectively. In Figure 10a, there is some deviation from linearity at the start of crack growth [6] (extreme right of the plots), however, the current procedure using PC reduces this significantly. In Figure 10b, there is noticeable curvature at both extremes. The linear regression lines fitted for the “steady stage growth” [3,6] displays a smaller slope for the crack length estimates from PD as a result the larger crack length prediction.



(a)



(b)

Figure 9: View of Crack Opening Angle in Specimen from Steel (a) 4840-2 and (b)3

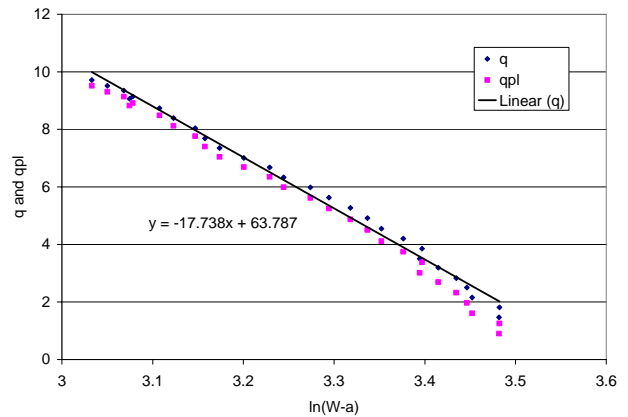


Figure 10a: Load Line Displacement (q) vs. $\ln(W-a)$ from the Test Presented in Figure 6 with Crack Length Estimates from Compliance

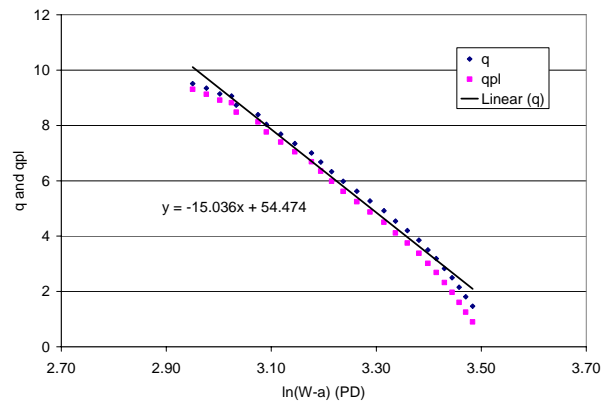


Figure 10b: Same Plot as Figure 10a, with Crack Length Estimates from PD

Using equation (1) the slope of the lines can be used to determine the CTOA [3,6]. Table 4 gives these values from triplicate specimens tested for steel 2, for the (B x 4B) size.

The CTOA is calculated by two methods:

- (i) Assuming a plastic rotation factor (r_{pl}^*) of 0.44 and the standard span (S) of 4W.
- (ii) Using the rotation factor derived from expression (2), i.e. (r_{pl}^*) of ≈ 0.6

DISCUSSION

The results presented for CTOA are discussed here in detail with the objective of critically evaluating the constancy of CTOA in the “steady state crack growth” regime as identified in the linear portions of the q vs. ln(W-a) plots [3,6]. The examples presented are representative of two steels (2 and 3) that were studied in detail using (B x 2B), (B x 4B) and (B x 6B), in that linear portions after a small non-linear region, as shown in Figure 10, was consistent. From equation (1) and the linear portion of Figure 10 it can be argued that the CTOA is constant when r_{pl}^* is constant. In conventional fracture toughness testing using standard (B x 2B) specimens this parameter is taken as 0.44 (ASTM E1290) and for non-standard three point bend specimens it has been assumed to be 0.4 [6] or 0.45 [9]. In the present work a rigorous analysis of this parameter was done using the non standard (B x 4B) and (B x 6B) size specimens, using expression (2). For the (B x 4B) size, r_{pl}^* was 0.61 ± 0.05 and for the (B x 6B) size 0.56 ± 0.03 . These are larger than the values reported, however, it is not known whether the standard values are relevant for CTOA testing, where the focus is on larger crack growth using three point bend specimens. The r_{pl}^* calculated here is based on dV_{pl}/dq_{pl} at a crack length that is about half of the full extension (Δa) in each test.

Table 4 describes the variation of the calculated CTOA from triplicate specimens for steel 2 using (B x 4B) specimens. It shows that the method of crack length estimation, compliance or DCPD, does not significantly affect the CTOA, however, the higher r_{pl}^* calculated from

expression (2) increases the CTOA values beyond the specimen to specimen variation. These findings apply for both steels and for (B x 4B) and (B x 6B) sizes where the four combinations of determining CTOA in Table 4 could be employed. Therefore, in Table 5, the average CTOA from the three different sizes of specimens are compared for one of the combinations.

Table 5: The Effect of Specimen (Ligament) Size on CTOA for Steels 4840-2 and 4840-3 Using One Method, i.e., Compliance for Crack Length Prediction and r_{pl}^* of 0.44.

Steel	Average CTOA (°)		
	(B x 2B)	(B x 4B)	(B x 6B)
4840-2	10.1	7.9 (11.1*)	6.3 (8*)
4840-3	14.5	13.5 (18*)	11.4 (14.3*)

* values from using the calculated, r_{pl}^* value

For steel 2, increasing the specimen ligament size appears to decrease the CTOA, while for steel 3 the drop is small. Figure 11a gives an example of the J-R plots obtained from the two non-standard specimens to evaluate the effect of the ligament length.

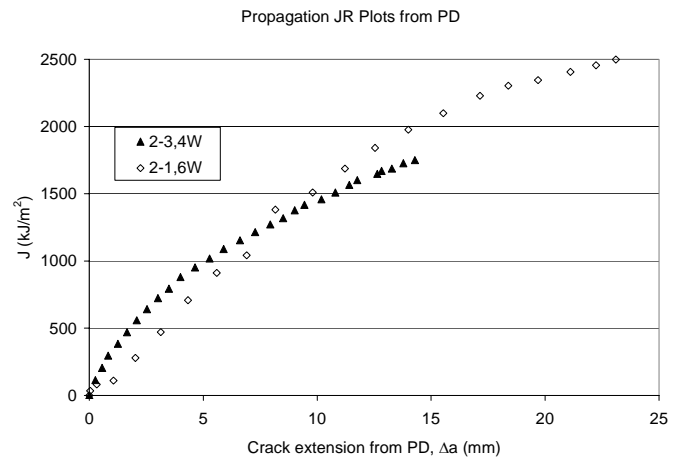


Figure 11a: J-R Plot for Steel 4840-2, Superimposing Results from Specimens with Two Ligament Lengths

Table 4: CTOA for Steel 2 for (B x 4B) Size, from Different Methods (Combinations of Crack Length (a) Predictions and Rotation Factor)

(a)	Elastic compliance			DCPD			
	Specimen	2-1,4Wch2	2-2,4Wch2	2-3,4Wch2	2-1,4Wch2	2-2,4Wch2	2-3,4Wch2
CTOA, (°)(i)		7.4	7.3	9.0	6.3	6.7	7.6
CTOA, (°)(ii)		9.8	12.4	11.2	8.4	11.3	9.5

Figure 11b is presented as an example to indicate specimen to specimen variation on the J-R plots and display similar resistance. The results in Figure 11a do not support a drop in CTOA with larger ligament length as indicated in Table 5, if there is a direct correspondence between the two measures of resistance to ductile fracture propagation (J and CTOA).

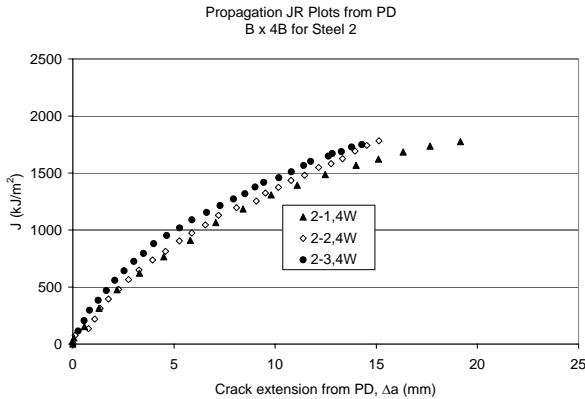


Figure 11b: J-R Plot for Steel 4840-2, Superimposing Results from (B x 4B) Specimens

In Table 6, the average CTOA determined for the four steels are compared with derived data from quasi-static (tensile) tests, to indicate that ϵ_f and A follow the ranking based on CTOA.

SUMMARY

The crack tip opening angle (CTOA) was investigated to evaluate its appropriateness as a measure of modern pipeline steel ductile fracture toughness. Results of fracture mechanics tests at quasi-static rate were analyzed to examine the constancy of CTOA with crack growth in four modern low C, low S chemistries and thermo-mechanically controlled processed (TMCP) steels. The linear relation observed between load line displacement (q) between ln (W-a) supports the concept of a constant CTOA during “steady state” crack propagation. When assuming the standard rotation factor of ≈ 0.44 the CTOA in this steady stage regime appears to be dependent on the ligament length of the SENB specimen; wider specimens show a tendency for lower CTOA. When the quasi-static CTOA is compared to tensile properties representing strain and strain energy to fracture, the rankings are similar. Further work is planned

to measure dynamic CTOA and evaluate the simple two specimen method.

ACKNOWLEDGMENTS

The project is funded by TCPL, IPSCO, Alliance Pipelines, Foothills Pipelines and STELCO. Contributions made by Dr. S. Tiku and Mr. C. Bayley of FTL are gratefully acknowledged.

REFERENCES

1. Eiber, R. J., Bubenik, T. A., and Maxey, W. A., December 1993, “Fracture Control Technology for Natural Gas Pipelines”; AGA NG-18 Report No. 208 for Project PR-3-9113.
2. Pussegoda, L.N., et.al, “An Interim Approach to Determine Dynamic Ductile Fracture Resistance of Modern High Toughness Pipeline Steels”, Submitted to IPC 2000.
3. Li, Z.F. and Turner, C.E., 1993, “Crack-Opening Angle and Dissipation-Rate Analysis of R-Curves for Side Grooved Pieces of HY 130 Steel in Bending”, Jour. Material Science, v.28, pp. 5922-5930.
4. Wang, , et.al, 1994, “An Engineering Fracture Parameter for Non-J Controlled Crack Growth”, Fatigue Fract. Engng. Mater. Struct., v.17, pp.469-477.
5. BS 7748: Part II: 1997.
6. Turner, C.E. and Kolednik, O., 1997, “A Simple Test Method for Energy Dissipation Rate, CTOA and the Study of Size and Transferability Effects for Large Amounts of Ductile Crack Growth” Fatigue Fract. Engng. Mater. Struct., v. 20, pp. 1507-1528.
7. Kirk, M.T. and Wang, Y-Y, 1995, “Wide Range CTOD Estimation Formulae for SE(B) Specimens”, Fracture Mechanics, 26th vol., ASTM STP 1256, W.G. Reuter and J.H. Underwood, eds., ASTM.
8. Gordon, J.R., 1986, “An Assessment of the Accuracy of the Method for Measuring Crack Growth Resistance Curves”, The Welding Institute, Cambridge, U.K. (325/1986).
9. Demofonti, G. et al, 1995, “Step by Step Procedure for the Two Specimen CTOA Test”, Pipeline Technology, ed. R. Denys, vol. II, Elsevier Science, pp. 503-512.
10. Martinelli, A. and Venzi, S., 1996, “Tearing Modulus, J-Integral, CTOA and Crack Profile Shape Obtained from the Load-Displacement Curve Only”, Eng. Fracture Mech., v.53, , pp. 263-277.

Table 6: Comparison of the Quasi-Static CTOA with True Fracture Strain (ϵ_f) and Area under the True Stress-Strain Curve (A)

Steel	Average CTOA ($^{\circ}$)			(ϵ_f)	A, (MPa)
	(B x2B)	(B x 4B)	(B x 6B)		
4840-1	17.3	n.a	n.a	1.60	2617
4840-2	10.1	7.9	6.3	0.92	1023
4840-3	14.5	13.5	11.4	1.46	1810
4840-6	21.8	n.a	n.a	1.67	2849

